(Received 16 October 2023, Accepted 28 November 2023, Scheduled 12 December 2023)

Wideband Capability in Embedded Stacked Rectangular Dielectric Resonator Antenna for X-Band Applications

Jihad Ben Yamoun* and Noura Aknin

Information Technology and Modeling Systems Research Group, Faculty of Sciences
Abdelmalek Essaadi University, Tetouan, Morocco

ABSTRACT: This paper introduces a novel design of an embedded stacked Rectangular Dielectric Resonator Antenna (RDRA). The antenna structure incorporates two distinct materials, namely PLA (Polylactic Acid) and Alumina, possessing dielectric constants of 3.45 and 9.9, respectively. A coaxial probe is employed to feed the antenna, enabling efficient signal transmission. The simulated results indicate the presence of two distinct resonance frequencies, which are 9.4 GHz and 10.6 GHz. Furthermore, the simulated antenna exhibits a maximum gain of 7.7 dB at 10.6 GHz, while demonstrating a wideband characteristic spanning approximately 22.7% of the frequency band between 8.75 GHz and 11 GHz on the measurement. The design and simulation of the RDRA are carried out using CST 2020 microwave studio, ensuring accurate and reliable results. The proposed antenna configuration is well suited for X-band applications such as radar and satellite systems.

1. INTRODUCTION

The first dielectric resonator antenna (DRA) was presented in 1983 [1], and this generation of antennas attracted the interest of researchers in order to develop this technology [2–4]. Therefore, from a performance point of view, there are true benefits. DRAs obtain significantly wider bandwidth and higher efficiency [5] than microstrip antennas, with low profile and compact size [6], low loss, light weight, and ease of excitation [7]. Moreover, this type of antennas can take different shapes as cylinder [1] and rectangle [7]. Moreover, DRA is characterized by the diversity of the materials used for the dielectric resonator. Indeed, the design and development of biodegradable antennas using PLA (Polylactic Acid) material has gained significant attention in recent years. These antennas offer numerous advantages, especially in applications where environmental sustainability and biocompatibility are crucial factors. Here are some key advantages of using PLA material for antenna design.

The biodegradability, the ease of fabrication as well, is considered biocompatible, making PLA antennas suitable for applications in medical devices, implantable devices, and wearable electronics. These antennas can be used for wireless communication in healthcare monitoring, biosensing, and other biomedical applications. PLA is also a relatively low-cost material compared to other specialty materials used in antenna fabrication. This makes PLA antennas an attractive option for cost-sensitive applications. PLA exhibits good thermal stability, allowing PLA antennas to withstand typical operating temperatures encountered in various applications.

The advantages of biodegradable antennas using PLA material make them a promising choice for environmentally conscious and sustainable wireless communication systems. Researchers continue to explore and refine the design and performance of PLA antennas to further enhance their capabilities and expand their applications [8–10]. And as well, the hybrid antennas serve to offer better bandwidth. Thus, DRA is a good candidate to design antennas for many applications satellites, 5G and terahertz [12–14].

Although varied Stacked and Embedded DRAs have been proposed last years, embedded dielectric resonators allow for efficient signal transmission and reception, making embedded antennas highly promising for applications in smart structures, wireless communication systems, and emerging technologies [15–20], with [18] showcasing the advantages of embedding technology in achieving desirable antenna performance for mm-wave applications. Unfortunately, they did not give many details about their effect on antenna performances resulting from what they offer to various physical parameters. While it is known that stacked DRAs have potential advantages over homogeneous DRAs, it has been difficult to formalize practical design procedures because of the lack of illustrative experiments investigating these parameter changes, and in [21] a wide bandwidth can be achieved with an array of 1×9 small DRAs by using stacked method the gain is 6.2 dB. Guo et al. proposed a dielectric resonator antenna which presents an impedance reaching 42% due to double annular-ring [22]. In [23], a designed antenna offers a wide input impedance in the ISM 2400 because of stacked rectangular dielectric resonator. It was found in [24] that two higher order modes of the whole dielectric resonator can be excited simultaneously, due to the embedded structure. The two degenerated modes lead to obtaining a larger band.

This study focuses on the design and development of a wideband embedded stacked rectangular resonator antenna, incorporating a feeding mechanism through an adjacent probe. The

* Corresponding author: Jihad Ben Yamoun (jbenyamoun@gmail.com).

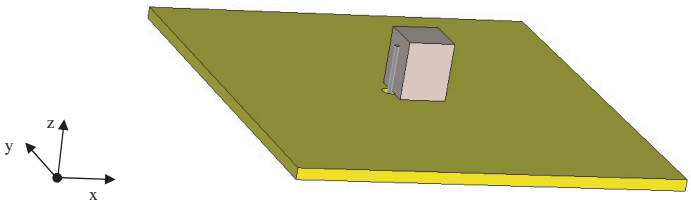

FIGURE 1. Three-dimensional view of homogeneous RDRA.

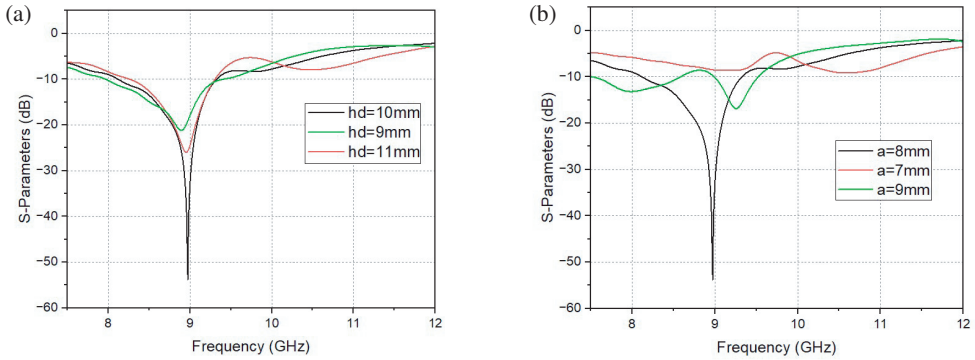

FIGURE 2. Simulated coefficient of reflection: (a) Sweep of the width and length of DRA h_d; (b) Sweep of the height of DRA h_d.

antenna structure is constructed using two distinct materials: Polylactic Acid (PLA) with a dielectric constant of 3.45, and Alumina with Warning: $\varepsilon_r = 9.9$. Through simulation using the CST 2020 EM simulator, the antenna exhibits two resonance frequencies at 9.4 GHz and 10.6 GHz, making it suitable for a wide range of applications. Notably, the antenna demonstrates an intriguing wideband capability, operating within the frequency range of 8.75 GHz to 11 GHz. This corresponds to a total fractional bandwidth of approximately 22.7%. Additionally, the antenna achieves a maximum gain of 7.7 dB, further enhancing its performance characteristics.

2. HOMOGENOUS DRA

2.1. Antenna Design

The dielectric waveguide model [25] is employed to examine the rectangular DRA. When the DRA is positioned on a ground plane, it stimulates TE modes. The resonant frequency of the primary mode, TE111, is determined using the subsequent equations [26]:

$$f_0 = \frac{c}{2\pi\sqrt{\varepsilon_r}}\sqrt{k_x^2 + k_y^2 + k_z^2} \quad (1)$$

$$k_x = \frac{\pi}{width}$$

$$k_z = \frac{\pi}{2 \times height}$$

$$k_y = \frac{2}{length}\tanh\left(\frac{k_{y0}}{k_y}\right) \text{ and } k_{y0} = \sqrt{{k_x}^2 + {k_z}^2}$$

The key parameters are defined as follows:

- k_x: Represents the wave number in the x-direction and is determined by the reciprocal of the width of the rectangular dielectric resonator antenna (DRA).
- k_z: Denotes the wave number in the z-direction and is determined by the reciprocal of twice the height of the DRA.
- k_y: Represents the wave number in the y-direction and is calculated based on the length of the DRA and the hyperbolic tangent function. Here, k_{y0} is the initial wave number in the y-direction.

Figure 1 illustrates a three-dimensional view of a homogeneous rectangular dielectric resonator antenna (DRA) consisting of Alumina with $\varepsilon_r = 9.9$. The antenna is positioned above an Aluminum ground plane measuring $60 \times 60 \times 2\,\text{mm}^3$. The dimensions of the DRA are as follows: a length of 8 mm, a width of 8 mm, and a height of 10 mm. The feeding method employed is an adjacent coaxial probe, ensuring efficient signal transmission and reception.

2.2. Results

A parametric study was conducted simultaneously for both width and length as shown in Figure 2, ranging from 7 mm to 9 mm with a step of 1 mm. Additionally, a second study was carried out for height, varying from 9 mm to 11 mm with a step of 1 mm. The optimal S_{11} was found to be achieved at a width and length $a = 8$ mm and a height $h_d = 10$ mm.

Figure 3(a) displays the simulated coefficient of reflection S_{11} of the antenna plotted as function of frequency. It is evident from the graph that the antenna exhibits a wideband characteristic spanning 12% of the frequency range. At a resonance frequency of 8.98 GHz, the antenna demonstrates a maximum return loss of -27.4 dB, efficient impedance matching. This is further supported by the voltage standing wave ratio (VSWR)

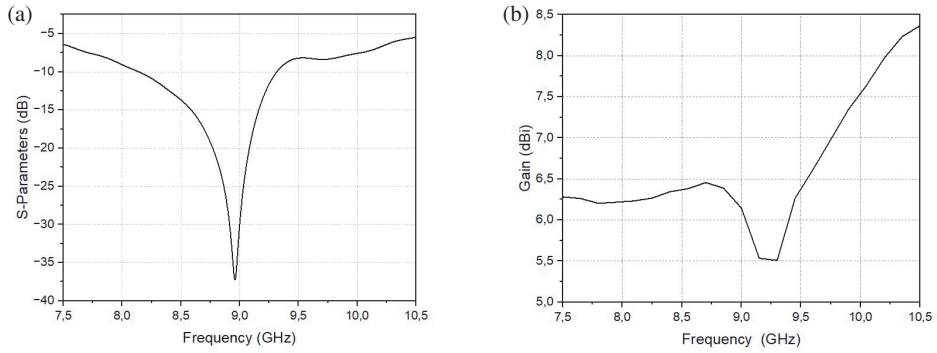

FIGURE 3. Simulated of the performances of homogeneous RDRA: (a) Coefficient of reflection Vs frequency; (b) Gain Vs frequency.

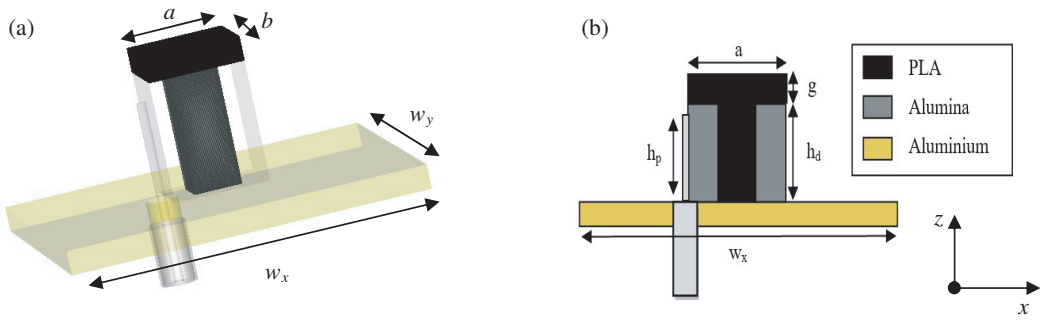

FIGURE 4. Embedded stacked rectangular DRA: (a) 3D view in CST; (b) Schematic of side view by cutting the structure in plan parallel to x axis on point $w_y/2$.

value of 1.04, confirming a high level of adaptation between the feeding method and the antenna structure.

Figure 3(b) showcases the gain performance of the antenna. At the resonance frequency of 8.98 GHz, the antenna achieves a gain value of 6.75 dBi. This emphasizes the antenna's ability to efficiently radiate and receive signals within the specified frequency range.

3. EMBEDDED STACKED DRA

The embedded stacked DRA represents a hybrid design that combines elements from both the stacked DRA and the core-plug embedded DRA. Among the various design variations studied, this configuration proved to be the most intricate and sophisticated. The insights gained from the stacked DRA and core-plug embedded DRA were influential in determining the most promising scenarios for optimal performance in cylindrical DRAs, as discussed in [28].

3.1. Proposed Antenna Architecture

For the evaluation of the proposed embedded stacked rectangular DRA, specific dimensions were chosen to match the geometry depicted in Figure 4. These dimensions were carefully selected to ensure the desired performance and characteristics of the antenna.

The dimensions of homogeneous DR made by Alumina presented before are: height $h_d = 10$ mm, width $a = 8$ mm, and length $b = 8$ mm above an Aluminum ground plane of height 2 mm, $w_x = 60$ mm, and $w_y = 60$ mm.

The dimensions of inner DR composed from PLA are: height $h_d = 10$ mm, width a′ $= 4$ mm, and length $b' = 4$ mm. The top layer is a PLA RD stacked above the two previous presented with a width $a = 8$ mm, length $b = 8$ mm and height $g = 3$ mm. The relative permittivity's are: for PLA $\varepsilon_{r-pla} = 3.45$ and the height of the pin's coaxial is optimized and fixed on the value $h_p = 8$ mm that shows the best adaptation.

The expression of the resonance frequency according to the method proposed by Marcatili for the waveguide method to solve Maxwell Equation (2) for rectangular dielectric waveguide [27] shows that when we decrease ε_r, the resonance frequency will increase:

$$f_0 = \frac{c}{2\pi\sqrt{\varepsilon_r}}\sqrt{kx^2 + ky^2 + kz^2} \tag{2}$$

3.2. Results and Discussion

The transition from the homogeneous Rectangular DRA to the Embedded Stacked DRA, as depicted in Figure 5, results in a notable shift in the operating frequency band. This shift is attributed to the inclusion of inner and top DRs composed of PLA, which possesses a relatively lower dielectric permittivity. As a consequence, the bandwidth of the antenna undergoes a significant improvement, expanding from 12% to 22.7% (measured). This enhancement classifies the antenna as wideband, as it nearly covers the entire X-band spectrum. Consequently, the Embedded Stacked DRA is highly suitable for various X-band applications, including radar and satellite communications.

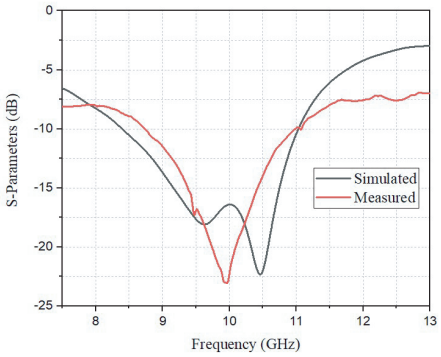

FIGURE 5. Simulated and measured Embedded Stacked DRA coefficient of reflection.

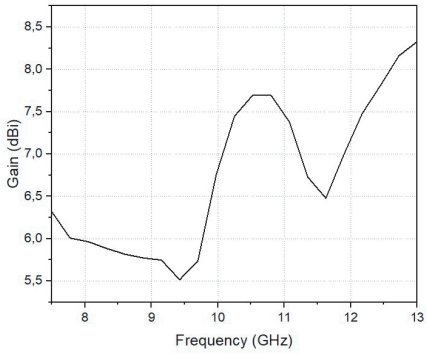

FIGURE 6. Simulated gain Vs frequency of the Embedded Stacked antenna.

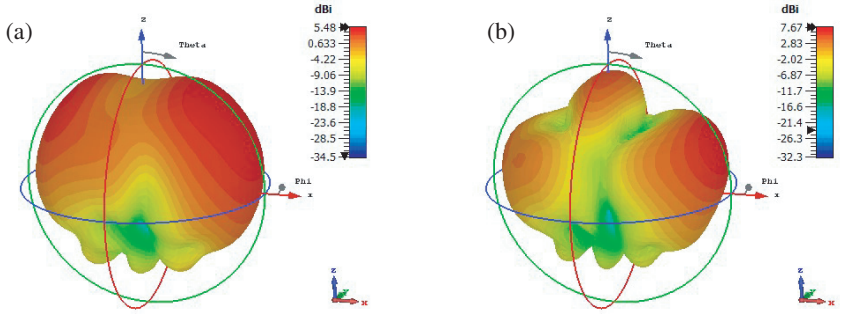

FIGURE 7. The performances of the Embedded Stacked antenna the three-dimensional radiation pattern: (a) 9.6 GHz; (b) 10.4 GHz.

Furthermore, the new antenna design exhibits the emergence of additional resonance frequencies. Specifically, the simulation shows that the antenna resonates at 9.65 GHz and 10.49 GHz, indicating the capability to operate at these frequencies and potentially support multiple communication channels or diverse signal requirements. Let's underline that the gain's value is also improved as illustrated Figure 6 and reaches 7.72 dBi at 10.49 GHz.

The observed performance improvements in the Embedded Stacked DRA can be attributed to the generation of two fundamental modes, which arise from the utilization of two different materials. Specifically, the Alumina material gives rise to the TE111 mode resonating at 9.65 GHz, while the PLA material contributes to the TE111 mode resonating at 10.49 GHz.

The expansion of the bandwidth in the Embedded Stacked DRA can be attributed to a decrease in the quality factor (Q-factor) of the antenna. This decrease in the Q-factor is a result of the electric field passing through materials with different permittivities. It has been documented in references [21] that this phenomenon contributes to the improvement of the antenna's bandwidth.

By incorporating materials with distinct permittivity values, the electric field distribution within the antenna structure is altered, leading to a broader operating bandwidth. This characteristic is particularly advantageous for applications that require a wide frequency coverage, as it enables the antenna to efficiently transmit and receive signals across a larger frequency range.

Figure 7 depicts the three-dimensional radiation pattern of the Embedded Stacked rectangular dielectric resonator antenna at two specific frequencies: 9.6 GHz and 10.4 GHz. The radiation pattern reveals that at 9.6 GHz, the antenna achieves a peak gain of 5.4 dBi, while at 10.4 GHz, the peak gain increases to 7.6 dBi. These values indicate the antenna's ability to concentrate and efficiently radiate electromagnetic energy in the desired direction at the respective frequencies.

Figure 8 showcases the simulated radiation patterns in the E-plane ($\varphi = 0°$) and H-plane ($\varphi = 90°$) for both frequencies. In the E-plane ($\varphi = 0°$), an almost omnidirectional pattern is observed for both frequencies. This indicates that the antenna radiates electromagnetic energy predominantly in the direction perpendicular to the antenna structure. In the H-plane ($\varphi = 90°$), at 9.6 GHz, the radiation pattern in the H-plane ($\varphi = 90°$) shows a larger beamwidth, indicating a broader coverage of radiation in different directions. On the other hand, at 10.4 GHz, significant radiation is observed in one specific direction and symmetrical broadside. This suggests that the antenna exhibits a directional radiation pattern in the $\varphi = 90°$ plane at this frequency.

The observed directional characteristics prompt an interesting consideration of the antenna's potential for generating shaped beams. The ability to tailor the radiation pattern to specific directions is crucial for various applications, such as beamforming in communication systems. In this context, we acknowledge the relevance of [29]. This work provides valuable insights into array pattern synthesis, including factors such

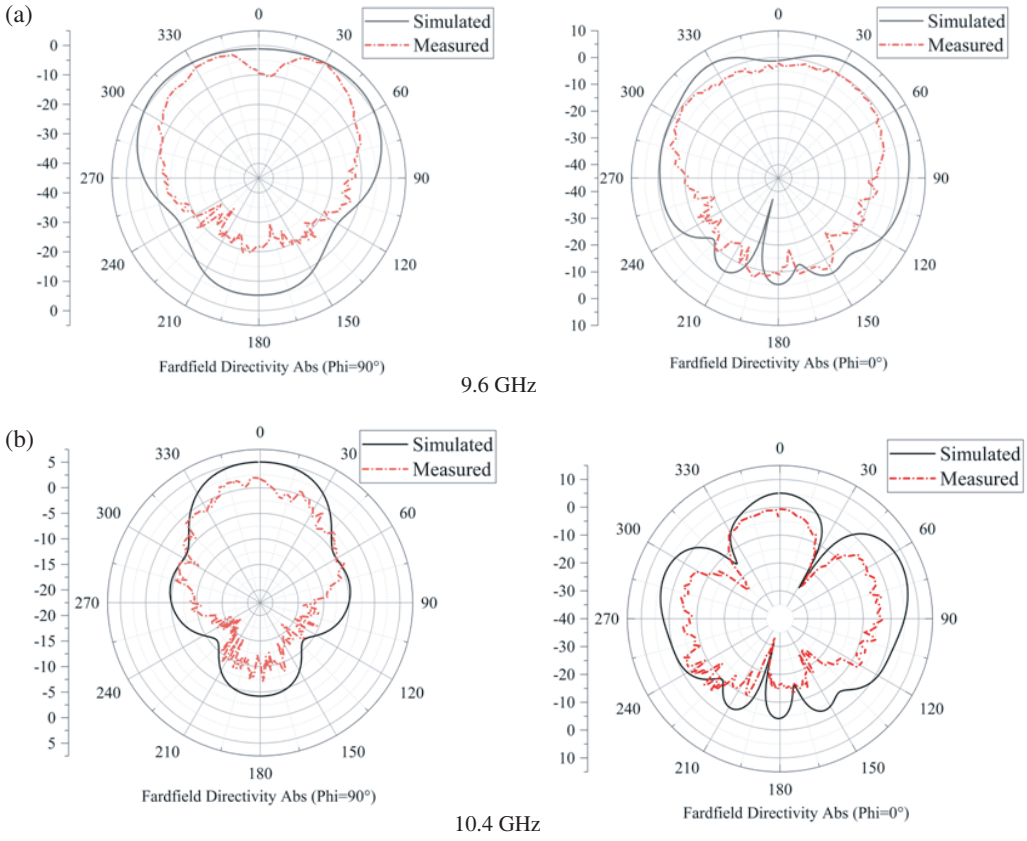

FIGURE 8. Simulated and Measured radiation patterns of the Embedded Stacked antenna on (a) H-plane and (b) E-plane: (a) 9.6 GHz; (b) 10.4 GHz.

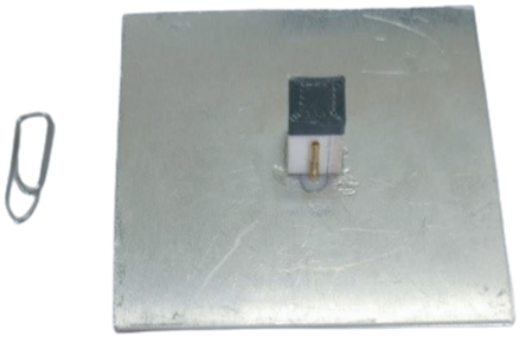

FIGURE 9. Three-dimensional view of antenna prototype.

as sparseness, mutual coupling, and mounting-platform effects. Further investigation inspired by this reference could shed light on the potential of our proposed antenna to generate shaped beams, contributing to its versatility in various communication and sensing applications.

Overall, the radiation patterns reveal the directional characteristics and beamwidths of the antenna at the specified frequencies, providing insights into the antenna's performance and coverage in different planes.

The experimental findings as illustrated in Figure 5 indicate that the fabricated antenna prototype shown in Figure 9 achieved a return loss of 10 dB over a wide bandwidth spanning from 8.75 GHz to 11 GHz. This translates to an impressive impedance bandwidth of 22.7%. Figure 8 highlights the antenna's ability to efficiently focus and radiate electromagnetic energy in the desired direction. Furthermore, clearly, the measured results align closely with the simulated outcomes, providing validation for the antenna's performance. However, certain discrepancies between the simulated and measured results exist due to fabrication imperfections, specifically related to the layer stacking. Despite these inconsistencies, the overall measurements affirm the antenna's effectiveness and underscore its potential for a range of applications. An Agilent N5222A Performance Network Analyzer is used to measure the result as observed in Figure 10.

TABLE 1. Comparison of the proposed Embedded Stacked DRA with recent works on bandwidth enhancement performance.

Reference	Frequency range (GHz)	Bandwidth (%)	Gain (dBi)	Dielectric constant
[17]	4.85–6.1	22.8	6.9–7.7	2.1 & 45
[18]	7.1–8.4	16.77	5.92	10 & 4.4
[19]	14.1–16.5	16.1	10.4	2.2
This paper	8.75–11	22.7	7.7	3.45 & 9.9

(a) (b)

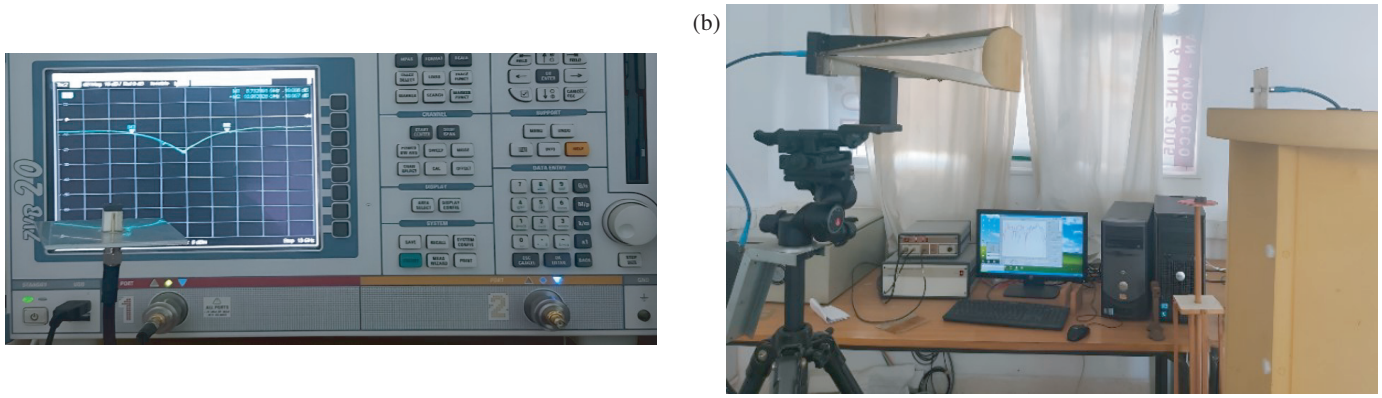

FIGURE 10. Measurement Bench for: (a) S_{11} Parameter; (b) Radiation Patterns.

Table 1 compares the performance of the proposed Embedded Stacked Dielectric Resonator Antenna (DRA) with three recent works on bandwidth enhancement in terms of frequency range, bandwidth percentage, gain, and dielectric constant. In comparison to references [17–19], it is notable that the proposed Embedded Stacked DRA in this study offers competitive performance, especially in terms of bandwidth and gain, positioning it favourably in the context of bandwidth enhancement for wireless communication applications.

4. CONCLUSION

In this paper, an Embedded Stacked Rectangular Resonator Antenna on polymere Polylactic Acid (PLA) and Alumina has been simulated and measured. An interesting working wideband: 8.75–11 GHz presents a total fractional bandwidth about 22.7% and all over the band obtains a high gain value. The maximum value of gain is 7.72 dBi. The obtained performances are adapted for x-band, radar, and satellite communications.

REFERENCES

[1] Long, S. A., M. W. McAllister, and L. C. Shen, "The resonant cylindrical dielectric cavity antenna," *IEEE Transactions on Antennas and Propagation*, Vol. 31, No. 3, 406–412, May 1983.

[2] Kishk, A. A., R. Chair, and K.-F. Lee, "Broadband dielectric resonator antennas excited by l-shaped probe," *IEEE Transactions on Antennas and Propagation*, Vol. 54, No. 8, 2182–2189, Aug. 2006.

[3] Jaoujal, A., A. Noura, and A. El Ahmed, "Wide-band rectangular dielectric resonator antenna for wireless applications," in *PIERS Proceedings*, 98–101, Marrakesh, Morocco, Mar. 2011.

[4] Denidni, T. A., Q. Rao, and A. R. Sebak, "Broadband l-shaped dielectric resonator antenna," *IEEE Antennas and Wireless Propagation Letters*, Vol. 4, 453–454, 2005.

[5] Kumar, A. V. P., V. Hamsakutty, J. Yohannan, and K. T. Mathew, "Microstripline fed cylindrical dielectric resonator antenna with a coplanar parasitic strip," *Progress In Electromagnetics Research*, Vol. 60, 143–152, 2006.

[6] Saed, M. and R. Yadla, "Microstrip-fed low profile and compact dielectric resonator antennas," *Progress In Electromagnetics Research*, Vol. 56, 151–162, 2006.

[7] Jaoujal, A., M. Younssi, N. Aknin, and A. El Moussaoui, "Wideband rectangular dielectric resonator antenna with two symmetrical gaps," *International Journal of Advanced Scientific and Technical Research*, Vol. 4, No. 2, 708–713, Aug. 2012.

[8] Kumar, P., D. Santanu, Utkarsh, S. Singh, and J. Kumar, "Investigation and development of 3D printed biodegradable PLA as compact antenna for broadband applications," *IETE Journal of Research*, Vol. 66, No. 1, 53–64, Jan. 2020.

[9] Marrocco, V., V. Basile, I. Fassi, M. Grande, D. Laneve, F. Prudenzano, and A. D'Orazio, "Dielectric resonant antennas via additive manufacturing for 5G communications," in *2019 Photonics & Electromagnetics Research Symposium — Spring (PIERS-Spring)*, 174–180, Rome, Italy, Jun. 2019.

[10] Kumar, A., K. Pragati, K. Pramod, K. Jitendra, and K. Amitesh, "Design and development of enhanced gain aperture coupled broadband biodegradable dielectric resonator antenna for WLAN applications," *Wireless Personal Communications*, Vol. 115, No. 2, 1525–1539, Nov. 2020.

[11] Ben Yamoun, J., A. Noura, and J. Achraf, "Low profile ultra wide band hybrid dielectric resonator antenna for emergent networks," in *2019 7th Mediterranean Congress of Telecommunications (CMT 2019)*, Fez, Morocco, IEEE, Oct. 2019.

[12] Sharma, A., K. Khare, and C. Shrivastava, "Dielectric resonator antenna for X band microwave application," *Research & Re-*

views, International Journal of Advanced Research in Electrical, Electronics and Instrumentation Engineering, Vol. 2, No. 6, 2013.

[13] Upender, P. and A. Kumar, "Quad-band circularly polarized tunable graphene based dielectric resonator antenna for terahertz applications," *Silicon*, Vol. 14, No. 10, 5513–5526, Jul. 2022.

[14] Ben Yamoun, J. and N. Aknin, "Broadband ring dielectric resonator antenna for satellite and 5G applications," *2020 International Symposium on Advanced Electrical and Communication Technologies (ISAECT)*, 1–3, 2020.

[15] Ki, T.-W. and S.-O. Pak, "Enhanced gain and miniaturisation method of stacked dielectric resonator antenna using metallic cap," *IET Microwaves Antennas & Propagation*, Vol. 13, No. 8, 1198–1201, Jul. 2019.

[16] Mani, S. and L. Edeswaran, "High gain multiband stacked DRA for WiMax and WLAN applications," *American Journal of Applied Sciences*, Vol. 14, No. 8, 779–785, 2017.

[17] Sun, W.-J., W.-W. Yang, P. Chu, and J.-X. Chen, "Design of a wideband circularly polarized stacked dielectric resonator antenna," *IEEE Transactions on Antennas and Propagation*, Vol. 67, No. 1, 591–595, Jan. 2019.

[18] Yang, M.-D., Y.-M. Pan, Y.-X. Sun, and K.-W. Leung, "Wideband circularly polarized substrate-integrated embedded dielectric resonator antenna for millimeter-wave applications," *IEEE Transactions on Antennas and Propagation*, Vol. 68, No. 2, 1145–1150, Feb. 2020.

[19] Ali, I., M. H. Jamaluddin, A. Gaya, and H. A. Rahim, "A dielectric resonator antenna with enhanced gain and bandwidth for 5G applications," *Sensors*, Vol. 20, No. 3, 675, Feb. 2020.

[20] Mauro, G. S., G. Castorina, F. A. Morabito, L. D. Donato, and G. Sorbello, "Effects of lossy background and rebars on antennas embedded in concrete structures," *Microwave and Optical Technology Letters*, Vol. 58, No. 11, 2653–2656, Nov. 2016.

[21] Wang, F., C. Zhang, H. Sun, and Y. Xiao, "Ultra-wideband dielectric resonator antenna design based on multilayer form," *International Journal of Antennas and Propagation*, Vol. 2019, 2019.

[22] Guo, Y. X., Y. F. Ruan, and a. X. Q. Shi, "Wide band stacked the compact circularly-polarized hollow rectangular dielectric resonator antenna with an underlaid quadrature coupler," *IEEE Transactions on Antennas and Propagation*, Vol. 59, No. 1, 288–293, Jan. 2011.

[23] Kumar, R. and R. K. Chaudhary, "Stacked rectangular dielectric resonator antenna with different volumes for wideband circular polarization coupled with step-shaped conformal strip," *International Journal of RF and Microwave Computer-aided Engineering*, Vol. 29, No. 6, e21667, Jun. 2019.

[24] Yang, M.-D., Y.-M. Pan, Y.-X. Sun, and K.-W. Leung, "Wideband circularly polarized substrate-integrated embedded dielectric resonator antenna for millimeter-wave applications," *IEEE Transactions on Antennas and Propagation*, Vol. 68, No. 2, 1145–1150, Feb. 2020.

[25] Legier, J. F., P. Kennis, S. Toutain, and J. Citerne, "Resonant frequencies of rectangular dielectric resonators," *IEEE Transactions on Microwave Theory and Techniques*, Vol. 28, No. 9, 1031–1034, 1980.

[26] Mongia, R. K., A. Ittibipoon, and M. Cuhaci, "Low-profile dielectric resonator antennas using a very high permittivity material," *Electronics Letters*, Vol. 30, No. 17, 1362–1363, Aug. 1994.

[27] Marcatili, E. A. C., "Dielectric rectangular waveguide and directional coupler for integrated optics," *Bell System Technical Journal*, Vol. 48, No. 7, 2071–2103, 1969.

[28] Walsh, A. G., S. Christopher, D. Young, and S. A. Long, "An investigation of stacked and embedded cylindrical dielectric resonator antennas," *IEEE Antennas and Wireless Propagation Letters*, Vol. 5, 130–133, 2006.

[29] Morabito, A. F., A. Di Carlo, L. Di Donato, T. Isernia, and G. Sorbello, "Extending spectral factorization to array pattern synthesis including sparseness, mutual coupling, and mounting-platform effects," *IEEE Transactions on Antennas and Propagation*, Vol. 67, No. 7, 4548–4559, Jul. 2019.